

## Spherically symmetric empty space and its dual in general relativity

Naresh Dadhich

Inter University Centre for Astronomy & Astrophysics, P.O. Box 4, Pune 411 007, India

**In the spirit of the Newtonian theory, we characterize spherically symmetric empty space in general relativity (GR) in terms of energy density measured by a static observer and convergence density experienced by null and time-like congruences. It turns out that the space surrounding a static particle is entirely specified by the vanishing of energy and null convergence density. The electrograv-dual<sup>1</sup> to this condition would be the vanishing of time-like and null convergence density which gives the dual-vacuum solution representing a Schwarzschild black hole with global monopole charge<sup>2</sup> or with a cloud of string dust<sup>3</sup>. Here the duality<sup>1</sup> is defined by interchange of active and passive electric parts of the Riemann curvature, which amounts to interchange of the Ricci and Einstein tensors. This effective characterization of stationary vacuum works for the Schwarzschild and NUT solutions. The most remarkable feature of the effective characterization of empty space is that it leads to new dual spaces and the method can also be applied to lower and higher dimensions.**

THE Newtonian gravitational field equation is given by  $\nabla^2 f = 4\pi G \rho$  and empty space is characterized by  $\rho = 0$ . It is well-known that the measure of energy is an ambiguous issue in GR primarily because of the inherent difficulty of non-localizability of gravitational field energy. However there is no difficulty in defining various kinds of energy density, signifying different aspects. The analogue of the Newtonian matter density is the energy density measured by a static observer and defined by  $\rho = T_{ab} u^a u^b$ ,  $u^a u_a = 1$ , where  $u_a = ((g)^{1/2}, 0, 0, 0)$  and  $T_{ab}$  is the matter-stress tensor of non-gravitational matter field. Then there is the convergence density experienced by time-like and null particle congruences in the Raychaudhuri equation<sup>4</sup>. They are defined as the time-like convergence density,  $\rho_t = (T_{ab} - \frac{1}{2} T g_{ab}) u^a u^b$  and the null convergence density  $\rho_n = T_{ab} v^a v^b$ ,  $v^a v_a = 0$ ,  $v_a = (1, (-g_{11}/g_{00})^{1/2}, 0, 0)$ . The energy density  $\rho$  refers to all kinds of energy other than the gravitational field energy, while the time-like and null convergence densities act as active gravitational charge densities. For a perfect fluid they are given by  $\rho_t = \frac{1}{2}(\rho + 3p)$  and  $\rho_n = \rho + p$ . It is important to recognize that these three densities represent different aspects of energy distribution and its gravitational linkage. They would thus in general not be equal. Obviously all the three can never be

equal unless space is flat. However  $\rho = \rho_t$  implies vanishing of scalar curvature (radiation),  $\rho = \rho_n$  indicates vanishing of pressure (dust) and  $\rho_t = \rho_n$  gives  $\rho = p$  (stiff fluid). It may be noted that the weak field and slow motion limit of the Einstein non-empty space equation is  $\nabla^2 f = 4\pi G \rho$ , while its limit in weak field and relativistic motion is  $\nabla^2 f = 8\pi G \rho_t$ .

In the following, we shall always refer  $\rho$  and  $\rho_t$  relative to a static observer, and  $\rho_n$  to radial null geodesic. This does, however, bring in a particular choice for the time-like and null vectors but the choice is well motivated by the physics of the situation. The radial direction is picked up by the 4-acceleration of the time-like particle, identifying the direction of gravitational force, and so is the static observer for measure of energy and time-like convergence densities.

The main question we wish to address in this note is, can we characterize empty space solely in terms of these densities?

The answer is yes for the space surrounding a static particle. This may in general be true for an isolated particle with some additional conditions which would specify the additional physical character of the problem. It is clear that any specification of empty space must involve density relative to both time-like and null particles. That means  $\rho_n$  must vanish in any case and in addition one or both of  $\rho$  and  $\rho_t$  must vanish. Of course there should be no energy flux,  $P^c = h^{ac} T_{ab} u^b = 0$ ,  $h^{ac} = g^{ac} - u^a u^c$ . It turns out that for spherical symmetry the effective equation for vacuum is  $\rho = \rho_n = P_c = 0$ , the solution of which would imply  $\rho_t = 0$  and vanishing of the all Ricci components. Thus vanishing of energy and its flux, and null convergence density is sufficient to characterize empty space for spherical symmetry as these conditions completely determine the unique Schwarzschild solution. The effective vacuum equation is less restrictive than the vanishing of the entire Ricci tensor.

What actually happens is, for the spherically symmetric metric in the curvature coordinates,  $P_c = 0$  and  $\rho_n = 0$  lead to  $R_{01} = 0$  and  $R_0^0 = R_1^1$  which imply  $g_{00} = f(r) = -g^{11}$ , and then  $\rho = 0$  means  $R_2^2 = 0$  which integrates to give the Schwarzschild solution completely with  $g_{00} = 1 - 2GM/r$  (we have set  $c = 1$ ). Thus instead of  $R_{ab} = 0$ , the less restrictive effective equation  $\rho = \rho_n = P_c = 0$  also equivalently characterizes empty space for a static particle. It is a covariant statement relative to a static observer and in the curvature coordinates it takes the form  $R_0^0 = R_1^1$ ,  $R_2^2 = 0 = R_3^3$ .

Since there are three kinds of density, which could vanish with two at a time in three different ways, it is then natural to ask what would the other two cases give rise to?

The first thing that comes to mind is to replace  $\rho$  by  $\rho_t$  in the effective equation to write  $\rho_t = 0 = \rho_n = P_c$ , which would imply  $G_0^0 = G_1^1$ ,  $G_2^2 = 0 = G_3^3$ . That is replacing Ricci by Einstein, which represents a duality relation between the two. Remarkably this duality transformation is implied at a more fundamental level by interchange of the active and

e-mail: nkd@iucaa.ernet.in

passive electric parts of the Riemann curvature<sup>1</sup>. (Active and passive electric parts of the Riemann curvature are defined by the double (one for each 2-form) projection of the Riemann tensor and its double (both left and right) dual on a time-like unit vector, and dual is the usual Hodge dual,  $*R_{abcd} = 1/2 \epsilon_{abmn}$ .) That is, interchange of active ( $E_{ab} = R_{abcd} u^c u^d$ ) and passive ( $R_{cd}^{mn} = *R^*_{abcd} u^c u^d$ ) electric parts implies interchange of the Ricci and Einstein tensors because contraction of Riemann gives Ricci while that of its double dual gives Einstein tensor. We have defined the electrogravity duality transformation<sup>1</sup> by interchange of the active and passive electric parts,

$$H_{ab} \rightarrow H_{ab}.$$

It is clear that  $r \leftrightarrow r_t, r_n \rightarrow r_n, P_c \rightarrow P_c$ .

Then the condition  $r_t = r_n = P_c = 0$  is electrograv-dual to the effective empty space equation given above, and its solution would give rise to the space dual to empty space. It can be easily verified that it integrates out to give the general solution given by  $g_{00} = -g^{11} = 1 - 8\pi G h^2 - 2GM/r$ , where  $h$  is a constant. This is an asymptotically non-flat non-empty space which reduces to the Schwarzschild empty space for  $h=0$ . At large  $r$ , the stresses it produces accord precisely to that of a global monopole of core mass  $M$  and  $h$  indicating the scale of symmetry breaking<sup>2</sup>. Alternatively it can exactly for all  $r$  represent a Schwarzschild black hole sitting in a cloud of string dust<sup>3</sup>. It is remarkable that here it arises as dual to empty space, i.e. dual to the Schwarzschild black hole<sup>1</sup>. A global monopole is supposed to be produced when global symmetry  $O(3)$  is spontaneously broken into  $U(1)$  in phase transition in the early Universe. The physical properties of this space have been investigated<sup>5</sup> and it turns out that the basic character of the field remains almost the same except for scaling of the Schwarzschild's values for the black hole temperature, the light bending and the perihelion advance<sup>6</sup>. The difference between the Schwarzschild solution and its dual can be demonstrated as follows. Both the solutions have  $g_{00} = -g^{11} = 1 + 2f$  with  $\nabla^2 f = 0$ , which would have the general solution  $f = k - M/r$ . The Schwarzschild solution has  $k=0$ , while the dual does not. This is the only essential difference between the two. It is this constant, which is physically trivial in the Newtonian theory, that brings in the global monopole charge, a topological defect.

Let us also consider the remaining possibility,  $r = r_t = P_c = 0$  which would in terms of the Ricci components imply  $R = 0, R^0_0 = 0$ . This integrates out to give the general solution,  $g_{00} = (k + \sqrt{1 - 2GM/r})^2, g_{11} = -(1 - 2GM/r)^{-1}$ , where  $k$  is a constant. It is an asymptotically flat non-empty space with the stresses given by

$$T^1_1 = \frac{2kGM/r^3}{k + \sqrt{1 - 2GM/r}} = -2T^2_2.$$

Obviously, these stresses cannot correspond to any physically acceptable matter field because  $r=0$ . On the other hand, the space-time unlike the dual solution remains asymptotically flat. It will admit a static surface only if  $k < 0$  at  $r_s = 2GM/(1 - k^2)$ . However  $r \geq 2GM$  always for  $g_{00}$  to be real. The region lying between  $r_s$  and  $2GM$  would define an ergosphere where negative energy orbits can, as for the Kerr black hole, occur. The Penrose process<sup>7</sup> can be set up to extract out the contribution of  $k$  only if it is negative. However we do not know the physical source for  $k$ .

On the other hand, when  $k > 0$ , there occurs no horizon and it can represent a wormhole<sup>8</sup> of throat radius  $r = 2GM$ . It is remarkable that it has the basic character of a wormhole which needs to be further investigated. Pursuing on this track, we are presently working out a viable wormhole model<sup>9</sup>.

This space is certainly empty relative to time-like particles as both  $r$  and  $r_t$  vanish but not so for photons as  $r_n \neq 0$ . At the least, it can be viewed as an asymptotic flatness preserving perturbation to the Schwarzschild field.

Further it is also possible to characterize the Reissner-Nordström solution of a charged black hole by  $r = r_t, r_n = P_c = 0$ , and the de Sitter ( $\Lambda$ -vacuum) space by  $r + r_t = 0, r_n = P_c = 0$ . In the Ricci components, the former would translate into  $R = 0, R^0_0 = R^1_1$ . This is clearly invariant under the duality transformation. It is a non-empty space with trace-free stress tensor. The de Sitter space is given by  $r + r_t = P_c = 0$ , which implies  $R_{ab} = \Lambda g_{ab}$ . Of course under the duality transformation the sign of  $\Lambda$  would change indicating that the de Sitter and anti de Sitter are dual of each other.

The next question is, could other empty space solutions representing isolated sources be characterized similarly?

It turns out that it is possible to characterize the NUT solution and its dual<sup>10,11</sup> in a similar manner. However an additional condition would come from the gravomagnetic monopole<sup>12</sup> character of the field. The most difficult and challenging problem would be to bring the Kerr solution in line. That is an open question and would engage us for some time in the future. The crux of the matter is to identify the additional condition corresponding to gravomagnetic character of the field and solving the resulting equations. Once that is achieved, our new characterization of vacuum would cover all the interesting cases.

In conclusion, we would like to say that it is always illuminating and insightful to understand the relativistic situations in terms of the familiar Newtonian concepts and constructs. Relating empty space to the absence of energy and convergence density is undoubtedly physically very appealing and intuitively soothing. The most remarkable aspect of this way of looking at empty space is that it gives rise, in a natural manner, to the new spaces dual to the corresponding empty spaces. The dual spaces only differ from the original vacuum spaces by inclusion of a topological defect, a global monopole charge.

Note that the characterization of empty space and its dual is by the covariant equations. Earlier the dual spacetimes<sup>1,13</sup> were obtained by modifying the vacuum equation, so as to break the invariance relative to the electrogravity duality transformation, in a rather ad-hoc manner. Now the effective vacuum equation has the direct physical meaning in terms of the energy and convergence density. This characterization could as well be applied in lower and higher dimensions to find new dual spaces. For example, in three-dimensional gravity the dual space represents a new class of black hole spaces<sup>14</sup> with a string dust matter field. For higher dimensions, the method would simply go through without any change for  $n$ -dimensional spherically symmetric space and the dual space would represent a corresponding Schwarzschild black hole with a global monopole charge. It can be further shown that a global monopole field in the Kaluza-Klein space can be constructed similarly<sup>15</sup> as dual to the vacuum solution<sup>16</sup>.

It is thus an interesting characterization of empty space which leads to new spaces dual to corresponding empty spaces.

1. Dadhich, N., *Mod. Phys. Lett. A*, 1999, **14**, 337.
2. Barriola, M. and Vilenkin, A., *Phys. Rev. Lett.*, 1989, **63**, 341.
3. Letelier, P. S., *Phys. Rev. D*, 1979, **20**, 1294.
4. Raychaudhuri, A. K., *Phys. Rev.*, 1955, **90**, 1123.
5. Harari, D. and Lousto, C., *Phys. Rev. D*, 1990, **42**, 2626.
6. Dadhich, N., Narayan, K. and Yajnik, U., *Pramana*, 1998, **50**, 307.
7. Penrose, R., *Riv. Nuovo Cimento*, 1969, **1**, 252.
8. Visser, M., *Lorentzian Wormholes: From Einstein to Hawking*, American Institute of Physics, 1995.
9. Mukherjee, S. and Dadhich, N., (under preparation).
10. Dadhich, N. and Nouri-Zonoz, M., (under preparation).
11. Nouri-Zonoz, M., Dadhich, N. and Lynden-Bell, D., *Class. Quantum Gravit.*, 1999, **16**, 1021.
12. Lynden-Bell, D. and Nouri-Zonoz, M., *Rev. Mod. Phys.*, 1998, **70**, 427.
13. Dadhich, N., in *Black Holes, Gravitational Radiation and the Universe* (eds Iyer, B. R. and Bhawal, B.), Kluwer, Dordrecht, 1999, p. 171.
14. Bose, S., Dadhich, N. and Kar, S., *Phys. Lett. B*, 2000, **477**, 451.
15. Dadhich, N., Patel, L. K. and Tikekar, R., *Mod. Phys. Lett. A*, 1999, **14**, 2721.
16. Banerjee, A., Chatterjee, S. and Sen, A. A., *Class. Quantum Gravit.*, 1996, **13**, 3141.

ACKNOWLEDGEMENT. I thank the referee for his constructive comments.

Received 6 December 1999; revised accepted 4 March 2000

## Comparative efficacy of Ayush-64 vs chloroquine in vivax malaria

Neena Valecha<sup>†‡</sup>, C. Usha Devi<sup>†</sup>, Hema Joshi<sup>†</sup>, V. K. Shahi<sup>\*</sup>, V. P. Sharma and Shiv Lal<sup>\*\*</sup>

<sup>†</sup>Malaria Research Centre, 22 Sham Nath Marg, Delhi 110 054, India

<sup>\*</sup>Central Council for Research in Ayurveda and Siddha, Anusandhan Bhavan, 61–65 Institutional Area, Opp. D-Block, Janakpuri, Delhi 110 058, India

<sup>\*\*</sup>National Anti Malaria Programme, 22 Sham Nath Marg, Delhi 110 054, India

**A phase II prospective comparative randomized clinical trial was conducted in patients of vivax malaria to compare the efficacy of Ayush-64 vs chloroquine. Ayush-64, a herbal formulation patented by Council of Ayurveda and Siddha was compared with chloroquine. Patients received an oral dose of either 1 g Ayush-64, three times a day for 5–7 days or a total dose of 1500 mg chloroquine over 3 days. Peripheral smears were examined everyday for 3 days or till they were negative and then weekly up to 28 days.**

**The results of the study showed that at day 28, only 23 of 47 (48.9%) patients in the Ayush group and all the 41 in the chloroquine group were cured ( $p < 0.05$ ). Even in these 23 patients in the Ayush group parasite clearance time was longer than chloroquine (3.16 vs 1.5 days). Both regimens were generally well tolerated. In conclusion, Ayush-64 in a dose of 1 g three times a day for 5–7 days is not as effective for treatment of vivax malaria, as standard chloroquine therapy.**

MALARIA is a major health problem in India. The annual incidence was between 2 and 3 million during the last decade<sup>1</sup>. The problem of drug resistance and treatment failures in *P. falciparum*<sup>2</sup> and recently in *P. vivax*<sup>3,4</sup> malaria using chloroquine has focused interest on new drugs/drug combinations/indigenous drugs or remedies.

Ayush-64 is a combination of four Ayurvedic drugs namely *Alstonia scholaris* R. Br. (aqueous extract of the bark – 1 part), *Picrorhiza kurroa* Royle (aqueous extract of the rhizome – 1 part), *Swertia chirata* Buch-Ham (aqueous extract of the whole plant – 1 part) and *Caesalpinia crista* Linn (fine powder of seed pulp – 3 parts)<sup>5</sup>. The ingredients after mixing are formulated into tablets of 500 mg each. The drug/formulation is patented and registered by Central Council for Research in Ayurveda and Siddha (CCRAS) and was reported to cure malaria<sup>5,6</sup>. Since the studies were conducted more than 15 years ago and susceptibility of parasites to drugs keeps changing, it was considered essential to evaluate the efficacy of the drug before introduction in the national programme. Moreover, in these studies, patients were included on the basis of clinical diagnosis of malaria and assessment criteria were not uniform<sup>5</sup>, therefore

<sup>†</sup>For correspondence. (e-mail: valecha@del3.vsnl.net.in)

the present comparative study was designed to confirm the antimalarial activity of Ayush-64.

The study was conducted at Malaria Research Centre (MRC), Delhi. The clinics at MRC and the National Anti Malaria Programme (NAMP) were selected for the study. Patients from 4 to 5 peri-urban villages and resettlement colonies visit these clinics. They belong to the low socio-economic status. It was a prospective comparative, open and randomized study. The randomization was done by using a simple random sampling table. Proven cases of vivax malaria seeking treatment at the clinics of MRC and NAMP were asked to volunteer for the study if they were 18–60 years of age, had asexual parasitaemia  $< 50,000/\mu\text{l}$ , were febrile or had recent history of fever within the last 48 h. Pregnant and lactating females and G-6 PD deficient subjects were not included in the study. Patients who had taken antimalarials within 7 days prior to enrollment in the study were also not included.

The study was approved by an ethical committee of MRC. Patients satisfying the inclusion criteria were enrolled after obtaining an informed written consent. Patients were randomly allocated to receive one of the two treatment regimens. One group received a total dose of 1500 mg chloroquine over 3 days followed by 15 mg primaquine daily for 5 days as standard therapy for vivax malaria. The other group received Ayush-64, 2 tablets of 500 mg each three times a day for 5 days. The patients in the Ayush group who did not respond, as evidenced by the presence of parasites in the peripheral smear, were given treatment for further 2 days and labelled as treatment failures if they remained positive. This dose was as per recommendation by NAMP and in accordance with the doses used in earlier studies<sup>5,6</sup>.

Patients were observed for at least 2 h after drug administration for vomiting. They were then followed-up as outpatients on day 1, 2, 3, 7, 14, 21 and 28 for clinical and parasitological cure. All the patients who became positive after smear being negative at day 7 were labelled as recrudescences. Haematology and blood chemistry were done on day 0 and day 7. A slide was considered negative only after 200 fields had been examined without finding a parasite. The antimalarial efficacy in both groups was compared using parasite clearance time (PCT), cure rate at day 28 and recrudescence rate as parameters. The technician involved in investigations was not aware of the treatment regimen of the patients. The statistical method used for comparing PCT was the *t*-test and the *z*-test was used for cure rate and recrudescence rate in the two groups.

Fifty-four cases of *P. vivax* were enrolled in the Ayush-64 group and fifty in the chloroquine group. Seven cases in the former (age 19–50 years) and nine in the latter (age 18–40 years) group were lost to follow-up before they had completed the 28-day observation period. Although the drop-out rate was similar in both groups, the reasons were different. In chloroquine group the drop-out was because patients left the study area after being smear negative and the

28-day follow-up could not be completed. In the Ayush group, 4 cases dropped out as they did not want to continue therapy after the third day while 3 left the study area. Patients randomized to the Ayush-64 and chloroquine groups had comparable baseline characteristics with respect to age, sex, duration of illness, initial parasite counts, clinical symptoms, etc. (Table 1).

In the chloroquine group ( $n = 41$ ) mean parasite clearance time was  $1.5 \pm 0.5$  days compared to  $3.16 \pm 2.4$  days in the Ayush-64 group ( $n = 31$  including recrudescence cases). The values were significantly different with  $p < 0.05$  (*t*-test). Similarly cure rate of 100% vs 48.9% in the chloroquine and Ayush groups, respectively was significantly different ( $p < 0.05$ ) from each other. Recrudescence rate in the chloroquine group was 0% as against 17% in the Ayush group ( $p < 0.05$ ).

In addition, clinical recovery was also slow in the Ayush group and general acceptability of the drug was poor. The patients complained about frequency and duration of dosing and size and quality of the tablet formulation. The course of parasitaemia in the two treatment groups is shown in Figure 1. Out of the 16 cases who were labelled as treatment failures in the Ayush group, three had to be referred to hospital due to deterioration of clinical condition and all responded to chloroquine therapy.

Both treatment regimens were generally well tolerated. There was no significant difference in pre- and post-treatment haematological or biochemical findings in both treatment groups. One patient of the Ayush group had generalized oedema and proteinuria but causality relationship could not be established since the patient was lost to follow-up. Three patients in the Ayush group complained of gastrointestinal disturbances, viz. nausea and diarrhoea.

In the recent past efforts are being made to revive indigenous systems of medicine. Ayush-64 has been previously shown to be effective as an antimalarial in animal experiments and clinical studies conducted by the CCRAS<sup>5,6</sup>. However, in experimental studies in rodent models, increase in survival time and not the parasite clearance was observed in the dose of 3 g per day for 4 days. In clinical studies an efficacy of 72–90% in vivax malaria was reported with the

**Table 1.** Curative efficacy of Ayush-64 and chloroquine

Parameter	Treatment groups	
	Ayush	Chloroquine
Total cases enrolled	54 (46 M + 8 F)	50 (35 M + 15 F)
Age	$29.40 \pm 9.04$ years	$30.46 \pm 10.25$ years
Parasitaemia on day 0	$0.25 \pm 0.26\%$	$0.31 \pm 0.32\%$
Dose of drug used	1 g tds $\times$ 5–7 days	1.5 g (base) over 3 days
Total cases completing 28 days	47	41
Cure rate	48.9%	100%
Recrudescence rate	17%	0
Parasite clearance time	$3.16 \pm 2.4$ days	$1.5 \pm 0.5$ days

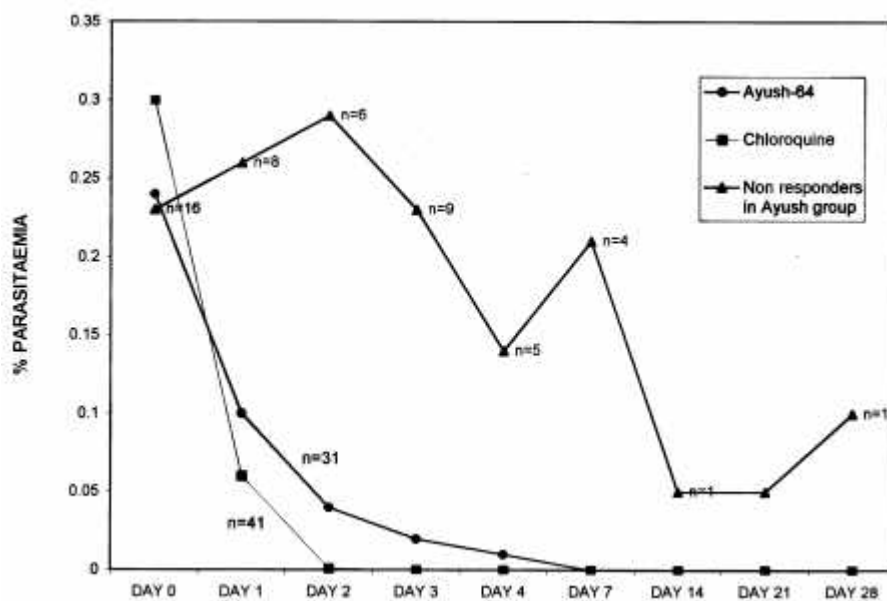


**Figure 1.** Course of parasitaemia in the two treatment groups. Data are arithmetic mean of parasitaemia.

dose of 3 g/day for 4–5 days. However, some of the cases were included on the basis of clinical diagnosis only.

Similarly Sharma *et al.*<sup>6</sup> have shown the efficacy of Ayush-64 with variable dose and duration of treatment to be 70%. In all the studies the total dose of drug has varied from 9 to 37 g. The frequency of administration varied from patient to patient. However, the total daily dose was not more than 3 g in any case.

In the present study a uniform dose schedule of 3 g per day for 5 days (15 g) extending to 7 days if needed (21 g) has been used.

A cure rate of less than 50% has been observed with Ayush-64 as against 100% with chloroquine. The latter drug was administered once a day only for 3 days and is therefore more acceptable and cost effective. It is evident from the present study that Ayush-64 does not have specific schizonticidal or gametocytocidal activity. Our results are supported by lack of antimalarial action in rodent and simian models even at dose of 3 g/kg (ref. 7). One of the ingredients of Ayush-64, i.e. *Alstonia scholaris* has also been shown to be devoid of specific antiplasmodial action<sup>8</sup>.

The drug does not appear promising as a primary drug for treatment of malaria in the present dose regimen. In addition to increasing morbidity, slow parasite clearance poses a threat of continuing transmission of the disease. And this,

therefore, is unlikely to be an alternative for chloroquine in vivax malaria. Considering the poor efficacy of the drug and risk of complications in falciparum malaria, further study in *P. falciparum* cases was not conducted.

1. Sharma, V. P., *Indian J. Med. Res.*, 1996, **103**, 26–45.
2. Sharma, R. S., Sharma, G. K. and Dhillon, G. P. S., in *Epidemiology and Control of Malaria in India*, 1996, pp. 87–93.
3. Garg, M., Gopinathan, N., Bodhe, P. and Kshirsagar, N. A., *Trans. Soc. Trop. Med. Hyg.*, 1995, **89**, 656–657.
4. Dua, V. K., Kar, P. K. and Sharma, V. P., *Trop. Med. Intl Health*, 1996, **1**, 816–819.
5. Anon, Report on Ayush-64, Central Council for Research in Ayurveda and Siddha, Government of India, 1987, pp. 1–128.
6. Sharma, K. D., Kapoor, M. L., Vaidya, S. P. and Sharma, L. K., *J. Res. Ayurveda Siddha*, 1981, **2**, 309–326.
7. Kazim, M., Puri, S. K., Dutta, G. P. and Narasimham, M. V. V. L., *Indian J. Malariol.*, 1991, **28**, 255–258.
8. Gandhi, M. and Vinayak, V. K., *J. Ethnopharmacol.*, 1990, **1**, 51–57.

**ACKNOWLEDGEMENTS.** We thank Mr A. R. Kotnala, Mrs P. Singhal, Mr Kesari Prasad, Mrs Alka Kapoor, Mrs Lalita Gupta and Mr Bhopal Singh for technical assistance.

Received 6 December 1999; revised accepted 4 March 2000

## Correlating dynamics to conformational properties: An analysis of atomic displacement parameters ( $B$ -values) in high-resolution protein structures

S. Parthasarathy and M. R. N. Murthy\*

Molecular Biophysics Unit, Indian Institute of Science, Bangalore 560 012, India

Atomic displacement parameters (ADPs) obtained by high resolution X-ray diffraction studies on single crystals of proteins represent the mean square displacement of atoms about their mean position. The relationship between the flexibility of the protein molecule and its conformation could be examined by a careful analysis of these ADPs. This communication presents the results of such a statistical analysis. It is shown that the ADPs are related to side chain conformations and are low for energetically favourable rotamers. Examination of the dependence of ADPs on non-planar distortions of the peptide geometry as represented by  $\omega$  angle reveals that the parameters depend on the direction of non-planar distortion. Those conformations with  $\omega$  larger than the ideal *trans* geometry ( $180^\circ$ – $190^\circ$ ) are more flexible when compared to those with  $\omega < 180^\circ$  ( $170^\circ$ – $180^\circ$ ). The average ADP of a peptide unit depends weakly on the Ramachandran angles at the corresponding Ca atom. Thus, the flexibility of different segments of the polypeptide appears to be sensitive to the conformation of the side chains as well as the main chain.

ADVANCES in high brilliance X-ray sources as well as computational procedures for the refinement of proteins at high resolution have provided accurate Atomic Displacement Parameters ( $B$ -values) for several proteins<sup>1,2</sup>. These structures have been analysed with reference to the atomic interactions responsible for protein stability, evolution, function, molecular recognition and principles that govern oligomerization. The information on protein flexibility and mobility available in terms of the ADPs obtained by protein high-resolution structure refinement, in contrast, has not been exploited to the same extent<sup>3–5</sup>. ADPs (or  $B$ -factors or temperature factors) deposited in the Protein Data Bank correspond to  $B = 8\sigma^2\langle u^2 \rangle$ , where  $\langle u^2 \rangle$  is the average of the mean square atomic displacements ( $\text{\AA}^2$ ) along the three coordinate axes and is given by  $(u_x^2 + u_y^2 + u_z^2)/3$ . These parameters represent the flexibility of protein atoms and are important factors controlling protein function and stability. The atomic displacement parameters determined for different proteins show large variations from one structure to another due to the differences in the static disorder and are also influenced by refinement procedures<sup>6</sup>. However, it has been shown that the frequency distribution of the  $B$ -factors expressed in units of standard deviation about their mean value at the Ca

atoms ( $B'$ ) are similar in protein structures<sup>7</sup>. This distribution could be accurately described as a superposition of two Gaussian functions. The frequency distribution for different amino acids could be used to deduce flexibility indices that are helpful in predicting mobile segments in proteins<sup>3,4,7</sup>. In this communication, we examine the dependence of ADPs on conformation of both the main chain and the side chain: (a)  $\phi$  representing the side chain rotamer, (b)  $\omega$  representing the peptide bond geometry, and (c) Ramachandran angles  $\phi$  and  $\psi$  representing main chain conformation. Generally, energetically unfavourable conformations are associated with high flexibility.

The representative list of protein structures<sup>8</sup> determined by single crystal X-ray diffraction methods and available in the Protein Data Bank<sup>9</sup> (November 1996 release) was chosen for the analysis. None of these structures has sequence identity greater than 25%. The resolution is better than 2.0  $\text{\AA}$  and the  $R$  factor is less than 0.2 for all the selected structures. The code numbers of the selected proteins are listed in Table 1.

For each of the selected structures, the  $B$ -values at the Ca positions were replaced by a normal variate as  $B'$ -factor,  $B' = (B_i - \langle B \rangle) / \sigma(B)$ , where  $\langle B \rangle = \Sigma B_i / N$ , where  $B_i$  is the  $B$ -value associated with Ca of the  $i$ th residue and  $N$  is the total number of residues in the protein, and  $\sigma^2(B) = \Sigma (B_i - \langle B \rangle)^2 / N$ . Normalization of  $B$ -values is required to compare  $B$ -values of different protein structures.

The  $\phi$  ( $\text{N-Ca-Cb-Cg}$  for most amino acids,  $\text{Og}$  for Ser and  $\text{Cg}$  for Ile) torsional angle for each side chain was computed as the angle between the planes containing  $\text{N-Ca-Cb}$  and  $\text{Ca-Cb-Cg}$  atoms, respectively. Following the usual convention, the angle was taken as the clockwise rotation of the  $\text{N-Ca}$  vector, looking down the  $\text{Ca-Cb}$  direction, required to bring it to overlap with the  $\text{Cb-Cg}$  vector. The rotamer conformation was represented as *gauche*<sup>-</sup> for  $-120^\circ < \phi < 0^\circ$ , *gauche*<sup>+</sup> for  $0^\circ < \phi < 120^\circ$ , and *trans* for  $120^\circ < \phi < 240^\circ$ . Frequency distribution of  $\phi$  was sampled at  $10^\circ$  intervals. Similarly, the  $\omega$  angle representing the deviation of the peptide geometry from a planar configuration

**Table 1.** PDB codes for the high-resolution structures selected for the analysis

131L	153L	1AMP	1ARB	1ARV	1ATL
1BAM	1BP2	1CCR	1CHD	1CHM	1CNS
1CSE	1CSH	1DAA	1DTS	1DUP	1DYR
1EDE	1FKJ	1FNC	1GOF	1GPR	1HMT
1IAE	1ISC	1KPT	1LCP	1LEN	1LTS
1MOL	1NFP	1NHK	1NAR	1OVA	1PBE
1PDA	1PGS	1PHG	1PTX	1REC	1REG
1RSY	1SAT	1SBP	1SNC	1SRI	1TAG
1TAH	1TCA	1THV	1TRY	1TTB	1TYS
1XNB	2ACQ	2ALP	2AYH	2AZA	2CBA
2CCY	2CDV	2CPL	2CTC	2END	2ER7
2GST	2HMZ	2HTS	2MNR	2NAC	2OLB
2PHY	2POR	2PRK	2SIL	2TGL	3CHY
3CLA	3COX	3DFR	3GRS	3PTE	3SIC
3TGI	4ENL	4GCR	4FGF	5RUB	5TIM
8ABP	8FAB	9RNT			

\*For correspondence. (e-mail: mrn@mbu.iisc.ernet.in)

was evaluated as the torsional angle  $\text{Ca}_i\text{-C}'_i\text{-N}_{i+1}\text{-Ca}_{i+1}$  (where  $i$  and  $i + 1$  represent consecutive residues).  $0^\circ$  and  $180^\circ$  in  $\omega$  correspond to ideal *cis* and *trans* peptide geometries, respectively. Sampling was at  $1^\circ$  intervals for statistical analysis. Ramchandran angles  $\phi$  and  $\psi$  representing the polypeptide conformation at each  $\text{Ca}$  atom were calculated as angles  $\text{C}'_{i-1}\text{-N}_i\text{-Ca}_i\text{-C}'_i$  and  $\text{N}_i\text{-Ca}_i\text{-C}'_i\text{-N}_{i+1}$ , respectively. Frequencies were counted in  $60^\circ$  bins of  $\phi$  and  $\psi$ .

The mean value of  $B'$ -factors corresponding to each rotamer and residue type was evaluated considering all the proteins. Similarly, the variation of mean  $B'$ -factors was

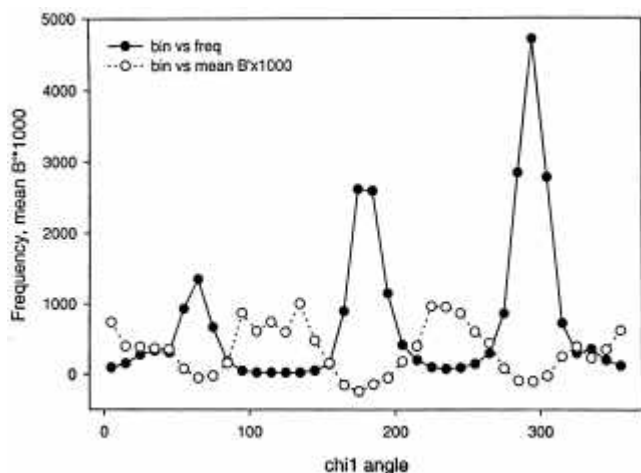


Figure 1. Frequency distribution of  $\psi$  values and dependence of mean  $B$ -factor on  $\psi$ .

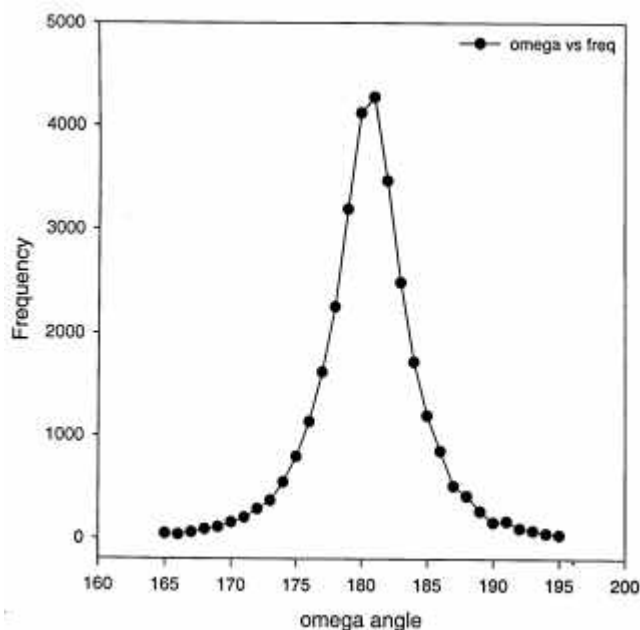


Figure 2. Frequency distribution of peptide non-planar distortion as represented by the dihedral angle  $\omega$

monitored as a function of  $\psi$  angle by grouping side chains into bins of  $10^\circ$ . Residues were also grouped in to different bins in the Ramchandran plot<sup>10</sup>. Even for fairly large bins, the population in certain regions of the Ramchandran map is sparse and hence the estimation of the mean  $B'$ -factors for these regions will not be statistically significant. An interval of  $60^\circ$  in  $\phi$  as well as  $\psi$  was found to provide sufficient number of residues in the bins corresponding to the allowed and partially allowed regions of the map.

Figure 1 shows the frequency distribution of side chain rotamers and their mean  $B'$ -factors for structures used in this study. The  $\psi$  distribution of side chain rotamers in the representative structures follows features that have been noted earlier<sup>11</sup>. For most residues, the preferred rotamers are *gauche*<sup>-</sup> and *trans* with somewhat less frequency in the *gauche*<sup>+</sup>. However, for amino acids branched at  $\text{Cb}$  the rotamer is either not well-defined or well determined. As these residues form only a small fragment of all the

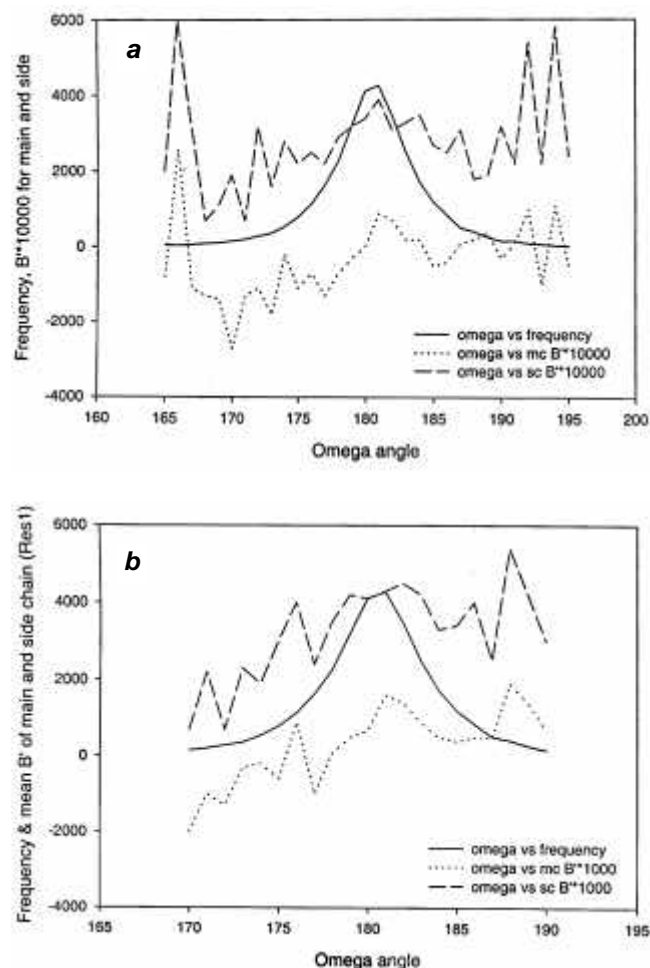


Figure 3. *a*, Variation of mean  $B'$ -factors of the main ( . . . ) and the side chain ( - - - ) of the  $\text{Ca}$  atom preceding the peptide bond as a function of peptide plane distortion  $\omega$  *b*, Variation of mean  $B'$ -factors of the main ( . . . ) and the side chain ( - - - ) of the  $\text{Ca}$  atom following the peptide bond as a function of peptide plane distortion  $\omega$

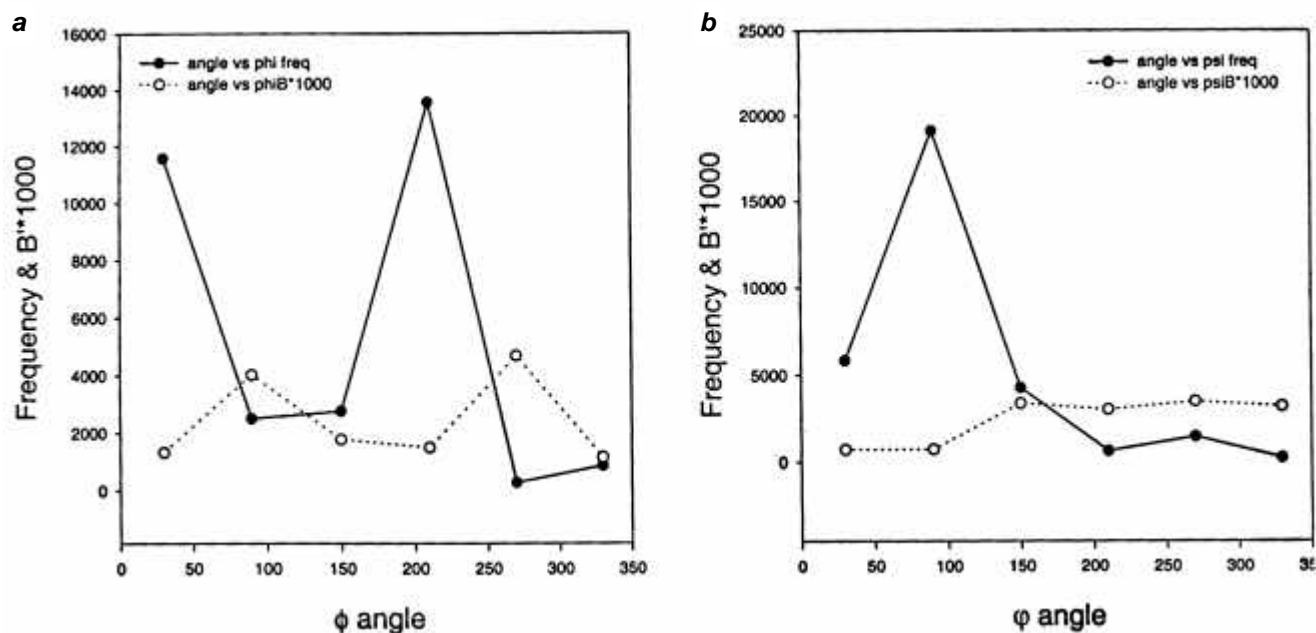
residues, they have not been excluded or treated independently in the present analysis. The peaks corresponding to the preferred rotamers have widths at half maximum of  $\sim 25^\circ$ . Although this spread might depend on the resolution at which the structures have been determined as well as the constraints used in refinement, the distribution shown in Figure 1 is typical<sup>11</sup>. The plot also shows the mean  $B'$ -factors for these conformational states. It should be noted that the frequency in bins mid way between preferred rotamers are low and hence the estimates of the mean  $B'$ -factors have large errors. The frequencies for intervals close to the preferred torsion angles are large and hence the estimated  $B'$ -factors are reliable. The  $B'$ -factors have clear minima at the preferred conformations of the side chains. It might also be noted that the most favoured torsion angle representing the *gauche*<sup>-</sup> form is less than  $300^\circ$ . The minimum in  $B$ -factor curve also occurs at this value. Similar observations have been made earlier<sup>11-13</sup>.

Figure 2 illustrates the frequency distribution of the  $\omega$  angle, representing out of plane deviation of the *trans* peptide unit about the C'-N bond and Figures 3 a and b show the variation of the mean  $B'$ -factor as a function of  $\omega$  for

both the preceding and succeeding residues, respectively. It is clear that the highest frequency occurs, not for the ideal *trans* geometry, but for  $\omega = 179^\circ$ . This deviation from the planarity of the peptide unit in proteins has previously been observed<sup>14</sup>. The distribution is nearly symmetrical about the preferred angle. On the contrary, the mean  $B'$ -factor appears to monotonically increase with increasing  $\omega$  in the range  $170^\circ$ - $190^\circ$ . It implies that the peptide group becomes more flexible when  $\omega$  increases from the value corresponding to the ideal *trans* geometry. The feature of larger  $B'$ -factors associated with  $\omega > 180^\circ$  are similar to the trend observed for rotamers – conformations with lower occupancy are associated with larger  $B'$ -factors. However,  $B'$ -factors continue to decrease when  $\omega$  changes to values lower than  $180^\circ$ , although the peptide changes to a higher energy state, as reflected by lower frequency of occurrence. Ramakrishnan and Balasubramanian<sup>15</sup> have shown that the area allowed in the Ramachandran diagram for non-glycyl residues reduces with increasing  $\omega$  in the range  $170^\circ$ - $190^\circ$ . Therefore, the reduction of  $B'$ -factor for non-planar distortions with  $\omega < 180^\circ$  might be due to the fact that the energy corresponding to the peptide geometry is determined by the

**Table 2.** Frequency of residues in bins of Ramachandran map and respective average  $B'$ -factors in brackets

4378 (-0.19)	6220 (-0.06)	733 (0.23)	16 (0.85)	138 (0.25)	91 (0.25)
709 (0.04)	1652 (-0.06)	55 (0.94)	47 (0.79)	39 (0.46)	11 (1.87)
309 (0.20)	1253 (0.32)	16 (0.65)	453 (0.23)	722 (0.38)	13 (0.00)
167 (0.32)	9611 (-0.09)	3382 (0.12)	20 (0.33)	348 (0.56)	22 (0.26)
36 (0.35)	110 (0.42)	64 (0.83)	28 (0.64)	34 (1.65)	9 (0.8)
244 (0.00)	243 (0.21)	15 (0.59)	75 (0.17)	177 (0.17)	114 (0.02)



**Figure 4.** Variation of the  $B'$ -factor as a function of (a)  $\phi$  and (b)  $\psi$ .

partial double bond character of the C'-N bond, while the flexibility might be related to the allowed area (lack of close contacts) of the Ramachandran diagram for the corresponding  $\psi$ . Similar trends are observed for the side chain and both the preceding and succeeding residues of the peptide bond.

Table 2 lists the frequencies of residues occurring in different bins of the Ramchandran plot sampled at 60° intervals in the structures selected for analysis. The numbers are consistent with the well-known features of the Ramachandran map<sup>16</sup>. The largest occupancy is found for the helical regions in the third quadrant and for strand regions in the second quadrant of the map. The  $B'$ -factors associated with the atoms  $N_i$ ,  $C_i\alpha$ ,  $C_i'$ ,  $N_{i+1}$  of all residues falling in the bins were averaged. The mean  $B'$ -factor of all Ca atoms was subtracted from this average. The values shown in Table 2 correspond to these. It is evident that the mean  $B'$ -factor is low for all cells where the occupancy is high. Since the frequency of occurrence depends on the energy corresponding to the particular cell, the flexibility is linked to the energy as observed for  $\phi$ . Similar observations were made for the  $B'$ -factors associated with the Ca atom alone. Thus the occurrence of a particular pair of Ramachandran angle has the effect of influencing the flexibility of the local segment of the polypeptide. Figure 4a illustrates the frequency and the mean  $B'$ -factor as a function of  $\phi$  (including all  $\psi$ ), while Figure 4b shows the same parameters as functions of  $\psi$  (including all  $\phi$ ). The correlation between high frequency and low flexibility is evident in these plots also.

Availability of a large number of well-determined three-dimensional structures of proteins makes possible studies on protein structure, function, evolution and dynamics. Preliminary examination of the ADPs determined during the course of high resolution X-ray structure determination of a set of unique proteins carried out in this communication clearly demonstrates that flexibility of the protein chain is dependent on conformation. Both main chain and side chain conformations appear to affect the mobility of residues. Residue mobility is minimum when the

side chain confirms to the most preferred rotamer. On the contrary, the mobility of the backbone depends asymmetrically on the departure of the peptide plane from ideal *trans* geometry. For non-planar distortions resulting from increasing  $\psi$  the flexibility increases. Peptides with  $\psi < 180^\circ$  tend to be less flexible although the distortions are not in the direction of reducing energy. This might be a consequence of a larger area of Ramachandran diagram allowed for peptides with  $\psi < 180^\circ$ . Flexibility of the polypeptide is also found to depend on the Ramachandran angles, partially allowed and disallowed regions correspond to larger  $B'$ -factors. Thus, the local flexibility of polypeptides appears to be influenced by main chain as well as side chain conformations.

1. Dauter, Z., Lamzin, V. S. and Wilson, K. S., *Curr. Opin. Struct. Biol.*, 1997, **7**, 681-688.
2. Merrit, E. A., *Acta Crystallogr. D*, 1999, **55**, 1109-1117.
3. Vihinen, M., Torkkila, E. and Riikonen, P., *Proteins: Struct. Funct. Genet.*, 1994, **19**, 141-149.
4. Karplus, P. A. and Schulz, G. E., *Naturwissenschaften*, 1985, **72**, 212-213.
5. Carugo, O. and Argos, P., *Acta Crystallogr. D*, 1999, **55**, 473-478.
6. Parthasarathy, S. and Murthy, M. R. N., *Acta Crystallogr. D*, 1999, **55**, 173-180.
7. Parthasarathy, S. and Murthy, M. R. N., *Protein Sci.*, 1997, **6**, 2561-2567; 1998, **7**, 525.
8. Hobohm U. and Sander C., *Protein Sci.*, 1994, **3**, 522-524.
9. Bernstein, F. C., Koetzle, T. F., Williams, G. J. B., Meyer, E. F. Jr. and Brice, M. D., *J. Mol. Biol.*, 1977, **112**, 535-542.
10. Ramachandran, G. N. and Sasisekharan, V., *Adv. Prot. Chem.*, 1968, **23**, 283-437.
11. Thanki, N., Umrana, Y., Thronton, J. M. and Goodfellow, J. M., *J. Mol. Biol.*, 1991, **221**, 669-691.
12. Dunbrack, R. L. Jr. and Karplus, M., *J. Mol. Biol.*, 1993, **230**, 543-574.
13. Carugo, O. and Argos, P., *Protein Eng.*, 1997, **10**, 777-787.
14. MacArthur, M. W. and Thornton, J. M., *J. Mol. Biol.*, 1996, **264**, 1180-1195.
15. Ramakrishnan, C. and Balasubramanian, R., *Int. J. Pept. Protein Res.*, 1972, **4**, 79-90.
16. Ramachandran, G. N., Ramakrishnan C. and Sasisekharan, V., *J. Mol. Biol.*, 1963, **7**, 95-99.

Received 14 October 1999; revised accepted 9 February 2000

## The plasmodia of *Physarum polycephalum*, an elegant system to demonstrate the importance of genome integrity in traversing the G2/M checkpoint of the cell cycle

P. R. Jayasree<sup>†</sup>, P. R. Manish Kumar<sup>†,\*</sup> and R. Vimala Nair<sup>\*\*</sup>

<sup>†</sup>Department of Biotechnology, University of Calicut, Calicut 673 635, India  
<sup>\*\*</sup>19/2084/A17 Express Tower, P. V. Sami Road, Calicut 673 002, India

**In this communication we show the usefulness of the plasmodia of *Physarum polycephalum* to demonstrate important concepts in cell cycle regulation, such as the need for an undamaged chromosomal DNA to allow the transition from late G2 to prophase (G2/M checkpoint). In *Physarum*, chromosomal DNA synthesis is confined approximately to the first one-third of the cell cycle which comprises the S phase, and rDNA and mitochondrial DNA are synthesized throughout the cycle except during mitosis and early S phase.**

**Taking advantage of these facts, DNA of the plasmodia was substituted with 5-bromo-2'-deoxyuridine at a concentration where it had no effect on DNA synthesis *per se* during different phases of the cell cycle before exposure to UV during late G2. A strong synergistic effect between BrdU and UV, in terms of mitotic delay, was observed only in plasmodia treated with the base analogue during the early S phase, thereby showing that the integrity of chromosomal DNA is an important prerequisite for the initiation of mitosis. It is suggested that this system is ideal for molecular level studies on this aspect of checkpoint operation.**

In eukaryotic cells, progression of cell cycle through different phases (G1, S, G2 and M) is controlled by a cell cycle control system. This system comprises brakes – the checkpoints – that can stop the cell cycle at two specific points – one in G1 before entry into S phase (G1/S checkpoint) and another in late G2, at the entry into mitosis (G2/M checkpoint). The checkpoints are signal transduction pathways whose effectors interact with cyclin/Cdk complexes to block cell cycle progression. A large number of studies have been carried out in yeast and mammalian cells to understand the molecular mechanisms operating at these points<sup>1-7</sup>.

Although the importance of chromosomal DNA in initiating mitosis<sup>8,9</sup>, and that of G2 phase as a period of surveillance to monitor the state of the nuclear DNA, before chromosomes are allowed to participate in mitosis and another cycle of reproduction, was envisaged since some years<sup>10</sup>, there has been a renewed interest now in under-

standing the mode of communication of chromosomal DNA with the signals which allow the cells to traverse the G2/M checkpoint. In the case of severe damage, G2 phase is also a time to activate programmed cell death<sup>11-13</sup>.

Entry into mitosis requires at least two events: activation of a mitosis promoting protein called Cdc2 by the Cdc25 phosphatase; and accumulation of active Cdc2 in the nucleus. The DNA damage checkpoint seems to block both these processes via pathways dependent on p53, a tumour suppressor protein, firstly by maintaining Cdc25 phosphatase in a phosphorylated form by protein kinase Chk1, followed by the binding of various 14-3-3 proteins<sup>14</sup> and the resultant export of this phosphatase out of the nucleus, thus preventing the Cdc2–cyclinB complex from getting activated. The other pathway operates via 14-3-3S protein which binds Cdc2–cyclin complex and sequesters it in the cytoplasm. There is evidence for the involvement of yet other factors and there could also be some amount of redundancy in the mechanisms operating at this checkpoint and further investigations are required to elucidate them<sup>15,16</sup>. Recent studies on cell-free extracts of *Xenopus* eggs which analysed the role of protein kinase Chk1 in checkpoint control show the similarity of this system with that of yeast and mammals<sup>14</sup>. There is also the proposal by Lydall and Weinert<sup>13</sup>, that damaged DNA could structurally inhibit mitosis, i.e. if condensed chromatin was a structural prerequisite for entry into mitosis, and damaged DNA could not be efficiently condensed.

Different types of perturbers have been used to analyse cell cycle regulation in the synchronously mitotic plasmodia of *Physarum polycephalum*<sup>17</sup>. It is known that UV irradiation during G2 inhibits RNA and protein syntheses<sup>18</sup>, and interferes with the organization of microtubular organizing centres<sup>19,20</sup> in this organism. Irradiation also leads to long mitotic delays<sup>18,21</sup>. It had also been observed that UV-irradiation causes decondensation of chromosomes in the plasmodia<sup>22</sup>. The higher susceptibility of S phase to UV in the plasmodia is also known<sup>21</sup>. Therefore, to single out the mitotic delaying effect of UV at the level of the integrity of chromosomal DNA *per se*, it is necessary to irradiate the plasmodia during very late G2, when chromosomal DNA synthesis is already completed and the chromosomes are condensed. It would also be ideal to use plasmodia whose DNA has already been sensitized to UV such that any effect is amplified.

The analogue of thymidine, 5-bromo-2'-deoxyuridine [BrdU] is readily incorporated into the DNA of the cells including that of the plasmodia of *Physarum*<sup>23</sup>. In the present experiments, it was thought desirable to accentuate the effect of UV on DNA by substituting it with this analogue, as BrdU incorporated DNA is known to be highly sensitive to radiation<sup>24</sup>. Along with BrdU, 5-fluorodeoxyuridine (FudR) and uridine (UR) were also supplied in the ratio 8:1:20, as was done earlier by McCormick *et al.*<sup>25</sup>. They had shown that FudR given in this ratio to the plasmodia of *Physarum* along with BrdU, would increase the incorpora-

\*For correspondence. (e-mail: prm@unical.ac.in)

tion of BrdU, into the DNA, because of FudR's known ability to block thymidine synthesis. UR in the above proportion was sufficient to prevent a decrease in the rate of RNA synthesis, caused by a breakdown of FudR to 5-fluorouracil and the consequent inhibition of UR biosynthesis. In the plasmodia of *Physarum* the chromosomal DNA synthesis is confined to the first one-third of the cell cycle which comprises the S phase (the G1 being absent). The cycle time varies from 8 to 12 h and the replication of the other DNA species (ribosomal DNA and mitochondrial DNA) takes place throughout the cycle except during mitosis and the early part of S phase<sup>26,27</sup>. In order to distinguish between the different DNA types, BrdU treatment was carried out at different phases of the cell cycle in surface plasmodia prepared as described below.

The McArdle strain (M3C) of *P. polycephalum* was grown as microplasmodia in shaken cultures in the dark at 24°C on a semi-defined medium (SDM)<sup>28</sup>. Mitotically synchronous surface (macro) plasmodia were prepared by the fusion of microplasmodia (0.4 ml packed suspension) on Whatman No. 40 filter paper<sup>29</sup> and grown in petri dishes supplied with SDM. Thereafter at regular intervals, synchronous postfusion mitoses (PFM) occur in these plasmodia.

Mitotic delay studies were carried out after irradiating (dose: 1400 Jm<sup>-2</sup>), both the BrdU-substituted (at different phases of the cell cycle) and unsubstituted plasmodial sectors at late G2 prior to the third PFM (details are given in legend to Figure 1), using a Philips 15 W germicidal lamp which had earlier been calibrated (dose rate: 7.18 Jm<sup>-2</sup> s<sup>-1</sup>) by actinometry<sup>30</sup>, and which emits approximately 90% of its UV energy at 2537 Å. DNA synthesis was evaluated by the radioisotope dilution technique of Devi and Guttes<sup>31</sup> (details are given in the legend to Figure 2), in the case of plasmodia substituted with BrdU during early S phase, where alone enhanced mitotic delay was observed.

The synergistic effect of UV and BrdU on mitotic delay was observed only in early S phase analogue-substituted category of plasmodia, in spite of increasing the treatment doses to 20 µg ml<sup>-1</sup> during late S phase or to 40 µg ml<sup>-1</sup> thereafter (Figure 1). Since mitochondrial and nucleolar DNA synthesis is seen throughout the cell cycle except during early S phase and mitosis<sup>26,27</sup>, the mitotic delay data (Figure 1) clearly indicate that BrdU incorporated into the chromosomal DNA of *Physarum* during the S phase of the cell cycle is the cause for the observed enhanced delay in the UV-irradiated system. The incorporated BrdU as such also causes some delays, particularly in those plasmodia treated with this analogue during early S phase.

The extra sensitivity seen in the plasmodia treated with BrdU during the early part of the S phase (significantly more than that seen with late S phase treatments) is understandable in view of the reported master-initiation of majority of the chromosomal replicons towards the early

part of the S phase and the increasing distances between regions in actual replication at later times in the S phase in the plasmodia of *Physarum*<sup>23</sup>. In fact, it is known that approximately 80% of the nuclear DNA of the plasmodia is replicated during the first 1 h 30 min of the S phase and much of the remaining 20% during the latter part of the S phase<sup>26</sup>. This way a higher rate of incorporation of BrdU into the chromosomal DNA is expected during early S phase.

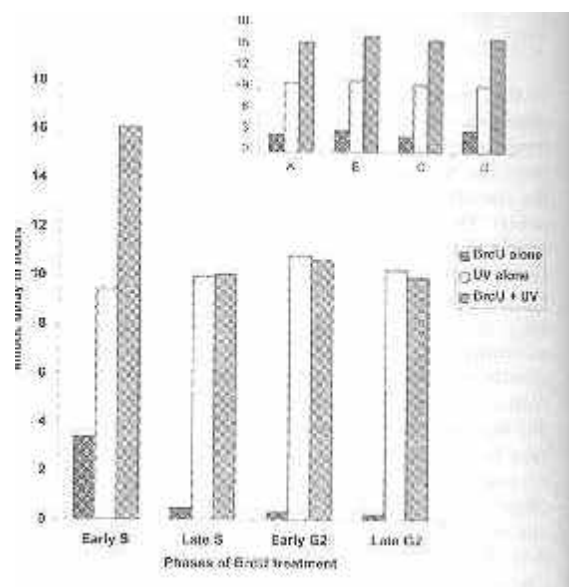


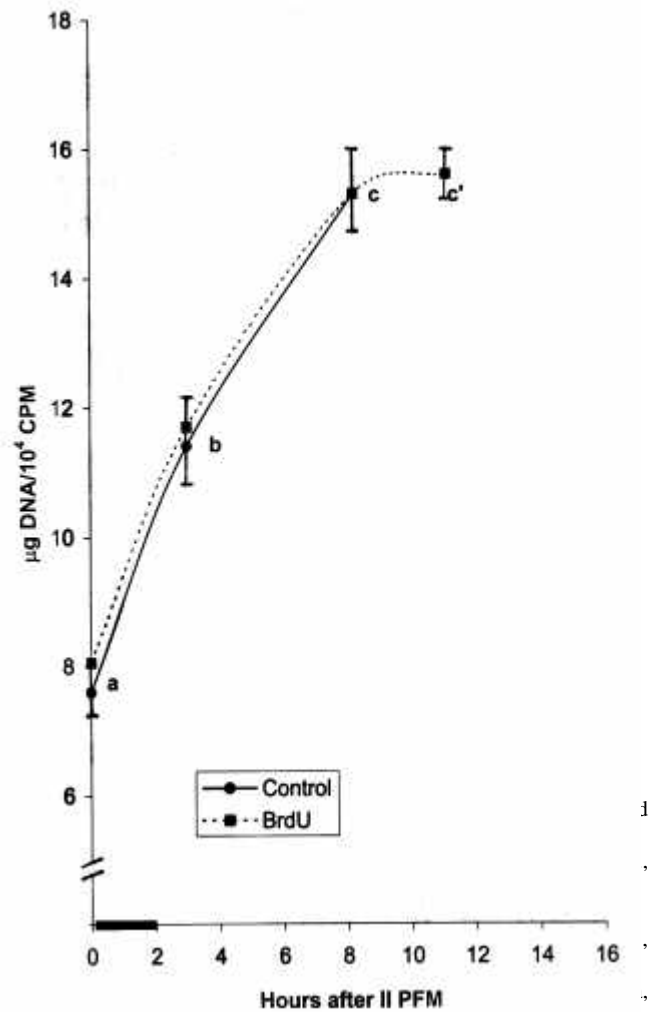
**Figure 1.** Effect of late G2, UV-irradiation on the mitotic cycle of BrdU substituted (at different phases of the cell cycle) plasmodia of *Physarum polycephalum*.

Each of the plasmodium in a set of sister plasmodia, made from pooled microplasmodial suspension, was cut into 4 sectors at the metaphase of the second PFM, and immediately after this, two of the sectors (sectors are synchronous with respect to each other) were pulse-treated for 2 h, during early S phase, with BrdU (5 µg ml<sup>-1</sup> of SDM). After the BrdU pulse and serial changes in fresh SDM to wash off the unincorporated analogue, both the control and the BrdU-substituted sectors were grown on fresh SDM till late G2. At approximately 30 min before their respective third PFM, one control (BrdU unsubstituted) and one BrdU-substituted sector from each plasmodium were UV-irradiated. The time of mitosis in all the sectors was noted and the mitotic delay due to the perturbations (i.e. BrdU alone, UV alone and BrdU + UV) was calculated with respect to their respective control sector (untreated and unirradiated).

Keeping the basic scheme of the experiment as above, 2 h BrdU pulse treatment was given during other phases of the cell cycle (late S, early G2 and late G2), followed by irradiation in late G2. In all these cases the mitotic delay due to the perturbations was calculated with respect to the respective control. Since 5 µg ml<sup>-1</sup> of BrdU was found to have no mitotic delaying effect when supplied during late S and G2 phases, still higher concentrations (20 and 40 µg ml<sup>-1</sup>) were used for these phases.

Values obtained from two plasmodia of each category have been averaged out and plotted in the bar diagram (Figure 1). Inset shows a projection of the values from four different plasmodia of the early S phase category, to highlight the extra sensitivity obtained here.

The enhancement of the G2-phase, UV-induced mitotic delay, because of S phase incorporation of BrdU into the chromosomal DNA of the plasmodia, is in agreement with the known extra vulnerability of BrdU-substituted DNA to UV<sup>32</sup>, apparently because of the production of DNA strand breaks and also DNA-DNA and DNA-protein cross-linkings in such systems<sup>33,34</sup>. Although G2-phase UV-irradiation as such is highly inhibitory to RNA and protein synthesis<sup>18</sup>, it is known from earlier studies that additional inhibitions were not observed because of BrdU incorporation<sup>35</sup>. At the concentration ( $5 \mu\text{g ml}^{-1}$ ) used to obtain extra mitotic delay, DNA synthesis was also not affected (Figure 2). As noted earlier, there was no enhancement in late G2, UV-induced mitotic delay, when BrdU treatment was carried out during the other phases of the cell cycle (Figure 1). The results of the present experiments clearly show that UV-induced alterations of chromosomal DNA, as late as G2-prophase transition period, can inhibit and postpone mitosis. This could well be because of the need for a signal based on the status of chromosomal DNA (undamaged) to start the process of mitosis<sup>8,9,12,13</sup>. It is already known that the DNA synthetic phase in the plasmodia is highly susceptible to UV-irradiation and maximum mitotic delay is obtained when irradiated during early S phase<sup>21</sup>. However, in this study we have been able to show the importance of the integrity of chromosomal DNA as such, in initiating the process of mitosis in this organism, which is quite independent of DNA synthesis. The idea behind these experiments was to show the elegance of the experimental system for demonstrations of this nature, and to suggest that the natural synchrony obtained here could be utilized in future molecular level investigations on checkpoints linking chromosomal DNA to G2/M transitions.



- Hartwell, L., *Cell*, 1992, **71**, 543-546.
- Kastan, M. B., Zhan, Q., El-Deiry, W. S., Carrier, F., Jacks, T., Walsh, W. V., Plunkett, B. S., Vogelstein, B. and Fornace, Jr. A. J., *Cell*, 1992, **71**, 587-597.
- Hunter, T., *Cell*, 1993, **75**, 839-841.
- Xiong, Y., Hannon, G. J., Zhang, H., Casso, D., Kobayashi, R. and Beach, D., *Nature*, 1993, **366**, 701-704.
- Nurse, P., *Cell*, 1994, **79**, 547-550.
- King, R. W., Jackson, P. K. and Kirschner, M. W., *Cell*, 1994, **79**, 563-571.
- Shiozaki, K. and Russell, P., *Nature*, 1995, **378**, 739-743.
- Lewin, B., *Cell*, 1990, **61**, 743-752.
- Weinert, T. A. and Hartwell, L. H., *Science*, 1988, **241**, 317-322.
- Lucke-Huhle, C., *Radiat. Res.*, 1982, **89**, 298-308.
- Furnari, B., Rhind, N. and Russell, P., *Science*, 1997, **277**, 1495-1497.
- O'Connell, M. J., Raleigh, J. M., Verkade, H. M. and Nurse, P., *EMBO J.*, 1997, **16**, 545-554.
- Lydall, D. and Weinert, T., *Curr. Opin. Genet. Dev.*, 1996, **6**, 4-11.
- Kumagai, A. J., Guo, Z., Emami, K. H., Wang, S. X. and Dunphy, W. G., *J. Cell. Biol.*, 1998, **142**, 1559-1569.

- Kumar, P. R. M. and Nair, V. R., *Biomed Lett.*, 1993, **48**, 137-143.
- Devi, V. R., Guttes, E. and Guttes, S., *Exp. Cell Res.*, 1968, **50**, 589-598.
- Jayasree, P. R. and Nair, V. R., *J. Biosci.*, 1991, **16**, 1-7.
- Funderud, S., Andreassen, R. and Haugli, F., *Nucleic Acids Res.*, 1978, **5**, 3303-3313.
- Kinsella, T. J., Mitchell, J. B., Russo, A., Aiken, M., Morstyn, G., Hsu, S. M., Rowland, J. and Glatstein, E., *J. Clin. Oncol.*, 1984, **2**, 1144-1150.
- McCormick, J. J., Marks, C. and Rusch, H. P., *Biochim. Biophys. Acta*, 1972, **287**, 246-255.
- Pierron, G., in *The Molecular Biology of Physarum polycephalum* (eds Dove, W. F. et al.), Plenum Press, New York, 1986, pp. 67-77.
- Evans, T. E., in *Cell Biology of Physarum and Didymium* (eds Aldrich, H. C. and Daniel, J. W.), Academic Press, New York, 1982, vol. 2, pp. 371-386.
- Daniel, J. W. and Baldwin, H. H., in *Methods in Cell Physiology* (ed. Presscott, D. M.), Academic Press, New York, 1964, vol. 1, pp. 9-41.
- Guttes, E. and Guttes, S., in *Methods in Cell Physiology* (ed. Presscott, D. M.), Academic Press, New York, 1964, vol. 1, pp. 43-54.
- Jagger, J. (ed.), *Introduction to Research in Ultraviolet Photobiology*, Prentice Hall, New Jersey, 1967.
- Devi, V. R. and Guttes, E., *Radiat. Res.*, 1972, **51**, 410-430.
- Murray, V. and Martin, R. F., *Nucleic Acids Res.*, 1989, **17**, 2675-2691.

33. Smith, D. W. and Hanawalt, P. C. (eds), *Molecular Photobiology: Inactivation and Recovery*, Academic Press, New York, 1969.
34. Kalia, V. K. and Jain, V., *Indian J. Exp. Biol.*, 1993, **31**, 224–230.
35. Jayasree, P. R., Ph D. thesis, Calicut University, Kerala, 1992.
36. Mittermayer, C., Braun, R. and Rusch, H. P., *Biochim. Biophys. Acta*, 1964, **91**, 399–405.

ACKNOWLEDGEMENTS. We thank Dr M. V. Joseph, Head and Co-ordinator, Department of Biotechnology, Prof. U. V. K. Mohammed, Head of the Department of Zoology, University of Calicut, and Prof. P. A. Wahid, Radiotracer Laboratory, Horticultural College, Thrissur for permission to use their departmental facilities for this work. Financial assistance to P.R.J. by the Council of Scientific and Industrial Research, Govt. of India is gratefully acknowledged.

Received 2 August 1999; revised accepted 13 January 2000

## ***Agrobacterium*-mediated genetic transformation and regeneration of transgenic plants from cotyledon explants of groundnut (*Arachis hypogaea* L.) via somatic embryogenesis**

**P. Venkatachalam<sup>†</sup>, N. Geetha, Abha Khandelwal, M. S. Shaila and G. Lakshmi Sita\***

Department of Microbiology and Cell Biology, Indian Institute of Science, Bangalore 560 012, India

<sup>†</sup>Rubber Research Institute of India, Kottayam 686 009, India

**An efficient transformation protocol was developed for groundnut (*Arachis hypogaea* L.) plants. Precultured cotyledons were co-cultured with *Agrobacterium tumefaciens* strain LBA 4404 harbouring the binary vector pBI121 containing the *uidA* (GUS) and *nptII* genes for 2 days and cultured on an embryo induction medium containing 0.5 mg/l NAA, 5.0 mg/l BAP, 75 µg/ml kanamycin and 300 µg/ml cefotaxime. The putatively transformed embryos were transferred to the medium with reduced kanamycin (50 µg/ml) for further development. Prolific shoots developed from these embryos on a MS medium containing 0.5 mg/l BAP and 50 µg/ml kanamycin with a transformation efficiency of 47%. The elongated kanamycin-resistant shoots were subsequently rooted on the MS medium supplemented with 1.0 mg/l IBA. The transgenic plants were later established in plastic cups. A strong GUS activity was detected in the putatively transformed plants by histochemical assay. Transformation was confirmed by PCR analyses. Integration of T-DNA into nuclear genome of transgenic plants was further confirmed by Southern hybridization with *nptII* gene probe. A large number of transgenic plants were obtained in this study. This protocol allows effective transformation and quick regeneration via embryogenesis.**

GROUNDNUT or peanut (*Arachis hypogaea* L.) is one of the principal economic oilseed legumes and is largely cultivated in many tropical and subtropical regions of the world. The seeds are mostly used to supply vegetable oil, carbohydrates and proteins for human as well as animal consumption. Crop improvement by conventional breeding in this important oilseed crop is not as rapid as envisaged to meet the demands of increasing population, especially in seed quality improvement and developing virus- and insect-resistant varieties. There is an urgent need to improve several commercially grown varieties in India and elsewhere. Tools of genetic engineering can be exploited as an additional method for introduction of agronomically useful traits into established cultivars. Major seed proteins of groundnut as well as of other leguminous crop species, are deficient in the essential sulphur containing amino acid

\*For correspondence. (e-mail: sitagl@mcbl.iisc.ernet.in)

methionine. Efforts are already made in this direction<sup>1</sup>. There are a few reports on transformation in some varieties of groundnut with marker genes<sup>2-4</sup> as well as one or two desirable genes like 2S albumin gene<sup>1</sup> and *Bt* gene<sup>5</sup>. However, to accomplish this and other genetic engineering objectives, an efficient gene delivery to isolated tissues and the subsequent regeneration of transformed plants must still be solved for commercially important, generally recalcitrant, groundnut cultivars<sup>1</sup>.

Although the transfer of foreign genes into the genome of groundnut calli was previously achieved with hypocotyl explants and other seedling explants, only a few of these reported the production of whole transgenic plants. This was mainly due to difficulties in transforming groundnut cells at sufficiently high frequencies. Although there are several approaches of developing transgenic plants, somatic embryogenesis has great potential in terms of high proliferation rates. Genetic transformation through somatic embryogenesis has not yet been reported in this oilseed crop. For successful introduction of desirable traits into the extensively cultivated varieties, efficient regeneration protocols as well as a gene delivery system need to be developed either by *Agrobacterium*-mediated gene transfer or the bombardment method. In this paper, we report successful transformation of groundnut by somatic embryogenesis with *uidA* and *nptII* genes.

Seeds of *A. hypogaea* L. cv. TMV-2 were obtained from the Agricultural College and Research Station, Tamil Nadu Agricultural University, Tiruchirapalli, India.

Seeds were surface disinfected with 5% Bavistin for 15 min, thoroughly washed with running tap water. Then they were sterilized with 0.1% (W/V) aqueous mercuric chloride solution for 7 min and washed with sterilized distilled water. Twenty seeds per plate were germinated aseptically in 90 × 15 mm petri dishes containing 40 ml of seed germination medium composed of the MS basal medium<sup>6</sup> consisting of 3% (W/V) sucrose and 0.8% (W/V) agar. Seeds and all *in vitro* plant materials were incubated at 25 ± 2°C under a 16 h photoperiod. Light was provided by cool white fluorescent lamps with an intensity of 60 μE m<sup>-2</sup> s<sup>-1</sup>. Cotyledon explants from 7-day-old seedlings were separated and used as explants for transformation experiments. Cotyledon explants were cultured on the embryo induction medium which consisted of the MS medium supplemented with 0.5 mg/l NAA and 1–10.0 mg/l BAP (MS1).

LBA 4404 strain of *A. tumefaciens* harbouring a binary plasmid pBI121 was used as the vector system for transfor-

mation. The vector map is given in Figure 1. Bacteria were maintained on LB (ref. 7) agar plates (1% W/V tryptone, 0.5% W/V yeast extract and 1% W/V sodium chloride, pH 7.0) containing 50 μg/ml kanamycin and 25 μg/ml rifampicin. For inoculation, one single colony was grown overnight on liquid LB at 28°C with appropriate antibiotics.

The explants were precultured for 2 days on the embryo induction medium prior to co-cultivation with bacterial culture collected at late log phase ( $A_{600}$  0.6). The cotyledons (300 explants) were gently shaken in the bacterial suspension for about 10 min and blotted dry on a sterile filter paper. Afterwards, they were transferred to the medium and co-cultivated under the same condition of the preculture period (16 h photoperiod of 60 μE m<sup>-2</sup> s<sup>-1</sup>) for 2 days at 25 ± 2°C. After co-culture, the explants were washed in the MS liquid medium, blotted dry on a sterile filter paper and transferred to the embryo induction medium (MS1) with antibiotics (75 μg/ml kanamycin and 300 μg/ml cefotaxime). Three subcultures are usually needed for the elimination of escapes. Later, the concentration of kanamycin was reduced to 50 μg/ml and completely devoid of cefotaxime.

After 4 weeks, the growing embryos were excised from the primary explant and subcultured into a fresh embryo proliferation medium containing 0.5 mg/l BAP and 50 μg/ml kanamycin (MS2). The green healthy shoots from the embryos were subjected to 2–3 more passages of selection by repeated excision of buds and their exposure to selective elongation medium (MS2). Healthy and elongated shoots were rooted in the MS medium containing 1.0 mg/l IBA but without kanamycin to facilitate rooting (MS3). Untransformed embryos do not withstand more than 25 μg/ml kanamycin. All experiments were carried out in ten replicates and the experiments were repeated at least three times, keeping all the parameters unchanged.

The β-glucuronidase (GUS) histochemical assay was used as a rapid way to detect the presence of the *uidA* gene (GUS) in the putative transformants as described by Jefferson *et al.*<sup>8</sup> using leaf segments in regenerated shoots from explants.

Presence of GUS and *nptII* was confirmed by PCR amplification of the *uidA* and *nptII* genes using two specific primer sequences. Plant DNA for PCR analysis was isolated as described by Edwards *et al.*<sup>9</sup>. Specific primers for *gus* (*uidA*) primer sequences (5'–3') were TTC GCG TCG GCA TCC GCT CAG TGG CA and GCG GAC GGG TAT CCG GTT CGT TGG CA. The *nptII* primer sequences (5'–3') were

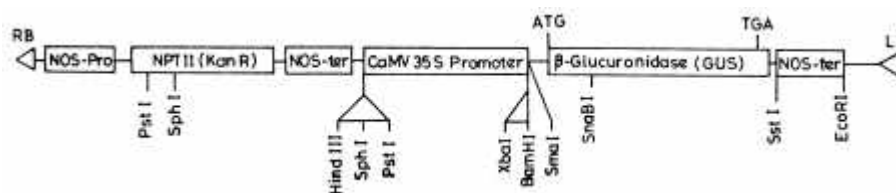


**Figure 1.** Diagrammatic representation of the pBI121 vector. The NOS-P, nopaline synthase gene promoter and NOS-T, nopaline synthase gene terminator signal control the expression of

GAG GCT ATT CGG CTA TGA CTG and ATC GGG AGG GGC GAT ACC GTA. Each PCR reaction was performed in 25 µl (total volume) of reaction mixture consisting of 10X reaction buffer, 150 ng DNA, 200 mM dNTPs, 25 mM MgCl<sub>2</sub>, 100 ng of each primer DNA and 1 unit of Taq DNA polymerase. PCR was carried out in a thermal cycler under the following conditions: 94°C for 4 min as preheating, then 35 cycles of 94°C denaturing for 1 min, 58°C annealing for 1 min and 72°C extension for 1 min and another 10 min at 72°C final extension for *uidA* gene detection, 94°C denaturing for 4 min as preheating, then 35 cycles of 94°C denaturing for 1 min, 55°C annealing for 1 min and 72°C synthesis for 1 min and 10 min at 72°C final extension for *nptII* gene detection. Amplified DNA fragments were electrophoresed on 1.2% agarose gel and detected by ethidium bromide staining, photographed under ultraviolet light.

Total genomic DNA was isolated from fresh leaves of transformed and untransformed (control) plants using the CTAB (cetyltrimethylammonium bromide) method. Southern blot hybridization analysis was carried out using standard procedures<sup>7,10</sup>. Ten µg of total genomic DNA from transgenic plants and untransformed control plant was digested with *HindIII*. 2 µg of plasmid DNA was digested with *SmaI* and *SacI* to release the *gus* fragment which was used to prepare the probe.

We have standardized plant regeneration in groundnut earlier by somatic embryogenesis<sup>11</sup>. After 3 weeks of culture, green multiple somatic embryos formed along the cut surface of the distal end of the cotyledons on the MS medium containing 0.5 mg/l NAA and 1–10.0 mg/l BAP. Among the various concentrations of BAP used, BAP 5.0 mg/l and NAA 0.5 mg/l (MS1) were found to be the best for maximum frequency of embryo formation (data not shown). This combination was routinely used for the transformation experiments. Each explant produced 20–30 somatic embryos (Figure 2 *a*), in some instances up to 60 embryos could be seen. Early separation shows the bipolar nature of the embryos (Figure 2 *b*) and these germinate with proper tap root if removed early (Figure 2 *c*). Histological observations also confirmed the nature of the bipolar embryos. If somatic embryos are not separated from the original cotyledon explants at an early stage, they tend to develop into profuse shoots (Figure 2 *d*) without root development. Embryos have to be separated for proper tap root development. However, separation of the embryos from clusters originating from the cotyledon explants was impossible without damaging the embryos as they fused with each other and to parent cotyledon explants, and have no discernible radicles. It was easier to allow the embryos to develop shoots for subsequent rooting by transferring to a medium with reduced BAP (MS2). This has been reported for groundnut<sup>12</sup> as well as eastern redbud<sup>13</sup> wherein multiple shoots developed from the somatic embryos. Single shoots can be excised from shoot clumps for rooting (MS3) to develop individual plants. Similar observations have been made with other legumes

like *Albizia lebeck*<sup>14</sup> and rosewood<sup>15</sup>. In general, somatic embryo morphology affects germination and plant conversion percentage in groundnut<sup>12,16</sup>. Multiple shoot formation from somatic embryos could be an alternative method of regeneration, especially if the somatic embryos are abnormal or there is a low percentage of germination.

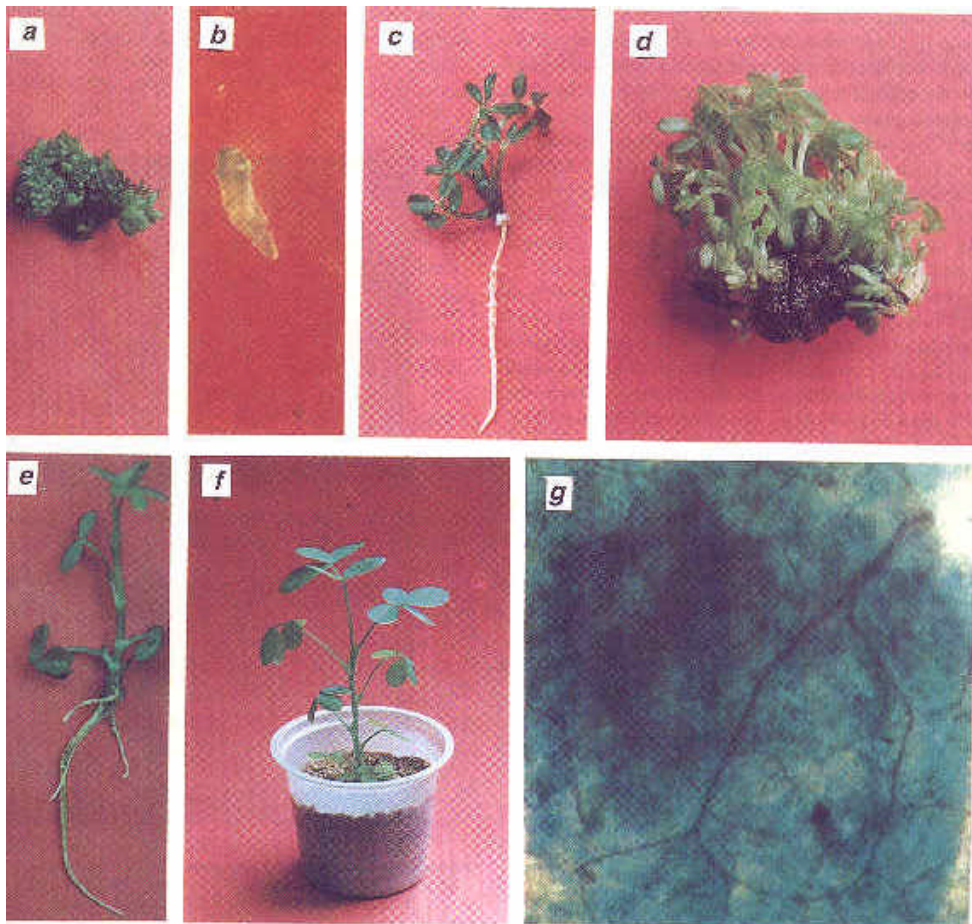
Kanamycin sensitivity of cotyledon explants was assessed prior to *Agrobacterium* transformation, to determine the concentration of kanamycin needed for effective growth of transgenic plants. At 50 µg/ml, kanamycin caused chlorosis and eventual necrosis in all explants by the end of the fourth week. Concentrations of 75 µg/ml and 100 µg/ml kanamycin completely inhibited embryo formation. Kanamycin concentration of 125 µg/ml and higher caused all explants to become necrotic by the third week of culture. Higher concentrations of 125 µg/ml kanamycin even killed almost all the cotyledon explants. In all previous reports of *Agrobacterium*-mediated transformation of groundnut, kanamycin concentration of 50–100 µg/ml was used in both the selection and regeneration medium<sup>2,3,17</sup>. In the present study, slightly higher kanamycin concentration (75 µg/ml) was used for the initial selection of transformants to prevent possible escapes. Subsequently, lower kanamycin concentration of 50 µg/ml was used to enhance the embryo proliferation. According to Pena *et al.*<sup>18</sup>, application of higher concentrations of the selection agent is the best way to eliminate the untransformed cells or organized tissues.

One of the critical factors in achieving high frequencies of transformation in groundnut is related to preculture of explants on the embryo induction medium prior to co-cultivation. Cotyledon explants were precultured for 0, 1, 2, 3, 4 and 5 days and transformation frequency was calculated by their embryo-forming ability in the selection medium (data not shown). When cotyledon explants were precultured on the regeneration medium for 2 days, the hypersensitivity response was reduced compared to co-cultivation with *Agrobacterium* without preculture. Preculture of the explants in the regeneration medium for 2 days prior to co-cultivation was found to be optimum for efficient transformation.

After selection through a two-day preculture, healthy cotyledons were infected and co-cultivated with *A. tumefaciens* LBA4404 harbouring pBI121 vector. During the initial two days on the non-selective embryo induction medium, all co-cultivated and control explant materials retained a healthy green colour. After transfer to the embryo induction medium with 75 µg/ml kanamycin and 300 µg/ml cefotaxime (selection medium) control explants and some of the co-cultivated explants became completely necrotic within 3–4 weeks. In contrast, control cotyledon explants maintained on non-selective embryo induction medium (without kanamycin) exhibited embryogenesis (86.6%) by the end of the fourth week in culture. Embryos formed directly around the distal end of the cotyledons without intervening callus and the maximum trans-

formation frequency was 47% (Table 1). The embryos were maintained by regular subculturing on the MS1 medium at 3-week intervals. After 3 passages on the MS1 medium, explants with somatic embryos were subcultured onto the MS2 medium for proliferation of shoots. On the other hand, controls did not require more than 4–6 weeks for transfer into the MS2 medium for proliferation. After prolonged culture period on the same medium, multiple shoots were regenerated from embryos on the MS2 medium (Figure 2 *d*). Similar results were also reported in eggplant<sup>19</sup>. Shoots developed from an individual embryo were sliced and subcultured on the MS medium with a low

level of BAP (0.2 mg/l) containing 50 µg/ml kanamycin for proliferation. The kanamycin concentration was lowered to 50 µg/ml at the third subculture to reduce antibiotic stress on the developing shoot buds. They were multiplied *in vitro* in the presence of kanamycin. Most of the transgenic clones appeared morphologically normal in comparison with the untransformed plants. The putative transformed shoots which attained 2–3 cm in length were excised and then transferred for rooting to the MS3 medium (Figure 2 *e*). Fifty plants were selected and these were transferred to the soil. Figure 2 *f* shows the well-established transgenic plant. The survival rate was 90–95%.



The transformation efficiency obtained in this study is as high as that reported earlier using groundnut leaf tissue<sup>2,3</sup>. Eapen and George<sup>2</sup> observed an average of 6.7% of shoot regeneration on the selection medium containing 50 µg/ml kanamycin. Cheng *et al.*<sup>3</sup> reported that the frequency of transformed fertile plants was 0.2 to 0.3% of the leaf explants inoculated. In the previous reports, transformation efficiency was low, as the explants were co-cultivated without preculturing. In the present study, an important factor which enhanced the transformation efficiency of groundnut was the 2-day preculture of the explants, which probably served to reduce wound stress and increased the number of competent cells at the wound site. A similar result was also reported in other species by Akama *et al.*<sup>20</sup> and Muthukumar *et al.*<sup>21</sup>. The results indicated that the efficiency of shoot regeneration was dependent on the explant type. Recent success in the production of transgenic plants using *Agrobacterium* in cowpea<sup>21</sup> and chickpea<sup>22</sup> was based on explants like hypocotyls, epicotyls and cotyledons. These results suggest that under the experimental conditions used in the present study cells of cotyledons may have commenced or 'shoot induction signals' and that the competence may

viously by Eapen and George<sup>2</sup> and Cheng *et al.*<sup>3</sup> in groundnut.

Presence of the *uidA* and *nptII* genes in the plant genome was confirmed by PCR analysis with specific primers using DNA from leaves. PCR analysis revealed that 0.53 kb *uidA* and 0.8 kb *nptII* DNA fragments amplified from genomic DNA of all putative transgenic plants. However, no *uidA* and *nptII* PCR products were seen for untransformed control plants. Figure 3a shows that all the samples of transgenic plants (lanes 4-9) gave the predicted size of DNA fragment of 0.53 kb of *uidA* gene. No band was detected in the DNA sample from an untransformed control plant (lane 3). The 0.53 kb DNA fragment was also amplified from the pBI121 plasmid as positive control (lane 2). DNA products with the expected size of 0.8 kb were amplified from total genomic DNAs of the putative transgenic plants (Figure 3b, lanes 5-11). These DNA fragments were not

**Table 1.** Transformation frequency of putatively transformed embryos from groundnut cotyledon explants on MS medium containing NAA (0.5 mg/l), BAP (5.0 mg/l), kanamycin (75 µg/ml) and cefotaxime (300 µg/ml)

Experiment	No. of explants co-cultured	No. of explants responded	Frequency of embryos	Average no. of embryos/cotyledon
Control*	75	65	86.6±4.3	65.0±3.7
Control**	86	0	00.0±0.0	00.0±0.0
Expt. 1	45	17	37.7±2.6	52.0±3.4
Expt. 2	36	15	41.6±3.8	48.0±3.1
Expt. 3	51	24	47.0±4.2	56.0±4.7
Expt. 4	39	17	43.5±3.6	32.0±2.8
Expt. 5	40	15	37.5±3.3	41.0±3.9

\*No co-cultivation, non-selective medium (without kanamycin).  
 \*\*No co-cultivation, selection medium (with 75 µg/ml of kanamycin).

vary in different groundnut explants.

The regenerated embryos or leaves were subjected to *in situ* GUS assay. The expression of *uidA* gene was verified by histochemical staining of the leaf of the transgenic plants. The *nptII* positive regenerants showed the typical indigo blue colouration of X-Gluc treatment, while the negative ones did not. Also, more than 45% of the regenerants were GUS positives. Young leaves were more densely stained than other tissue of the plant (Figure 2g). This seems to be a typical expression pattern of the CaMV 35S promoter regulated *uidA* gene in young tissues<sup>8</sup>. Leaf tissues from untransformed plants did not show GUS activity. These results and the extensive GUS expression in tissues, clearly demonstrate the stability of the inserted genes in the transformed plants. GUS expression was also reported pre-

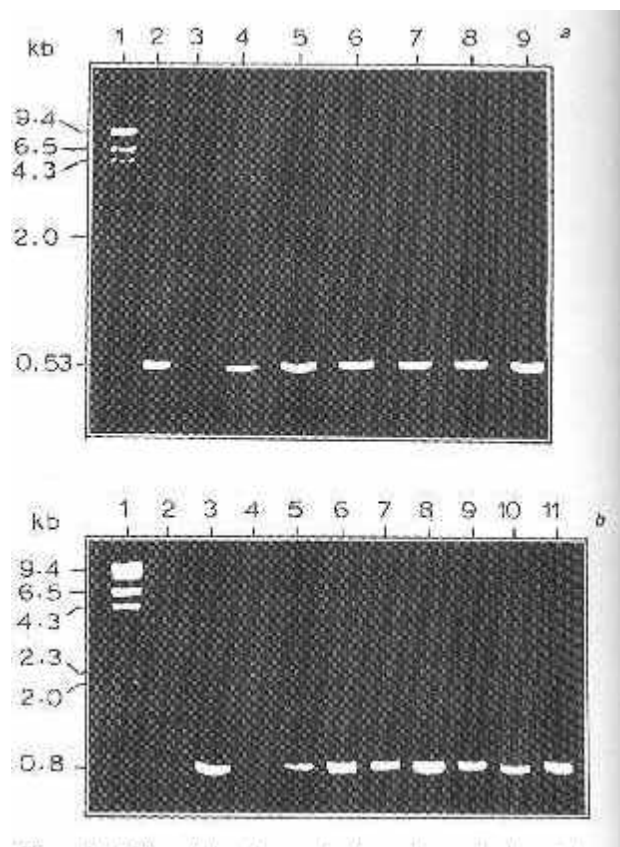


**Figure 3.** PCR analysis of transgenic shoots by amplification of the *uidA* (GUS) and *nptII* genes from total plant DNA extracts. *a*, Detection of the *uidA* (GUS) gene. Lane 1, DNA size marker; lane 2, Plasmid pBI121 (positive control); lane 3, Untransformed plant (negative control); lanes 4-9, Transformed plants; and *b*, Detection of the *nptII* gene. Lane 1, DNA size marker; lanes 2, 4, Untransformed plants (negative control); lane 3, Plasmid pBI121 (positive control); lanes 5-11, Transformed plants.

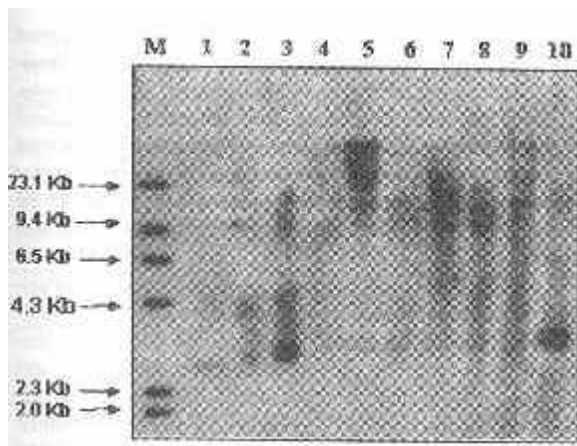


**Figure 4.** Southern blot analysis of transgenic groundnut plants previously identified by PCR analysis. Total genomic DNA (10 µg) digested with *Hind*III was hybridized with random primed  $\alpha^{32P}$  labelled *GUS* probes. Lane M, Labelled DNA size marker; lanes 1–10, Genomic DNA from independent lines of transformed plants.

detected in the untransformed control plant (Figure 3 b, lanes 2, 4). As a positive control, the *nptII* gene products were also amplified from the pBI121 plasmid (Figure 3 b Lane 3). Based on the resistance to kanamycin and PCR detection, presence of both *uidA* and *nptII* genes was confirmed in the transgenic groundnut plants. In the previous reports on transgenic groundnut plants obtained by micro-projectile bombardment<sup>1,23</sup> and *Agrobacterium*-mediated transformation<sup>2,24,25</sup> foreign gene products were not analysed by the PCR method.

The integration of the *gus* reporter gene into the transformed plant genomic DNA was further confirmed by Southern blot hybridization analysis. The genomic DNA from randomly selected GUS positive transgenics and one untransformed control plant was digested with *Hind*III which cuts at only one site located between the *uidA* (GUS) and *nptII* genes in the T-DNA insert of pBI121 plasmid. The *gus* gene was used as a probe. The *gus* DNA probe hybridized to DNA from transgenic plants (Figure 4) showed integration at different positions ranging from 2.5 kb to 23 kb. Few lines have shown single integration (lanes 1–4) and others have shown multiple integration (lanes 5–10). The DNA from the untransformed control plant did not show any signal (data not shown); the result indicated that the *gus* gene was integrated into the groundnut genome. A similar type of multiple copies of gene integration with the groundnut genome was reported by Ozias-Akins *et al.*<sup>26</sup> and Cheng *et al.*<sup>3</sup>

With the exception of the report by McKently *et al.*<sup>17</sup>, transformation frequencies for groundnut appear to be substantially lower in other reports of transformation. In this study protocol modification in the form of kanamycin concentration and preculture treatment substantially enhanced the transformation efficiency in groundnut and may be a major reason for the higher frequency obtained in this study

compared to the other reports on *Agrobacterium*-mediated transformation of this species. The results presented also demonstrate a simple and highly efficient system for producing peanut somatic embryos from cotyledon explants. The system does not require maintenance of embryogenic callus or apical meristem excision as in most previous procedures on genetic transformation of peanut, which are labour-intensive techniques. Moreover, in many cases the use of these explant materials results in the production of sterile plants and/or somaclonal variants. In the present study fertile plants were obtained. In addition, transformation was done via *Agrobacterium* and not by particle bombardment as was done in most of the previous reports which is an expensive method compared to *Agrobacterium*-mediated transformation. The protocol can be used efficiently for the introduction of more desirable genes and is currently being used for producing transgenic plants with desirable genes.

- Lacorte, C., Aragao, F. J. L., Almeida, E. R., Mansur, E. A. and Rech, E. L., *Plant Cell Rep.*, 1997, **16**, 619–623.
- Eapen, S. and George, L., *Plant Cell Rep.*, 1994, **13**, 582–586.
- Cheng, M., Jarret, R. L., Li, Z., Xing, A. and Demski, J. W., *Plant Cell Rep.*, 1996, **15**, 653–657.
- Wang, A., Hanli, F., Singsit, C. and Ozias-Akins, P., *Physiol. Plant.*, 1998, **102**, 38–48.
- Singsit, C., Adang, M. J., Lynch, R. E., Anderson, W. F., Wang, A., Cardineau, G. and Ozias-Akins, P., *Transgenic Res.*, 1997, **6**, 169–176.
- Murashige, T. and Skoog, F., *Physiol. Plant.*, 1962, **15**, 473–497.
- Sambrook, J., Fritsch, E. F. and Maniatis, T., *Molecular Cloning: A Laboratory Manual*, Cold Spring Harbor Laboratory Press, 1989, Second edn.
- Jefferson, R. A., Kavanagh, T. A. and Bevan, M. W., *EMBO J.*, 1987, **6**, 3901–3907.
- Edwards, K., Johnstone, C. and Thompson, C. C., *Nucleic Acids Res.*, 1991, **19**, 1349.
- Ben-Meir and Vainstein, A., *Sci. Hortic.*, 1994, **58**, 115–121.
- Venkatachalam, P., Geetha N., Abha Khandelwal, Shaila, M. S. and Lakshmi Sita, G., *Curr. Sci.*, 1999, **77**, 269–273.
- Chengalrayan, K., Mhaske, V. B. and Hazra, S., *Plant Cell Rep.*, 1997, **16**, 783–786.
- Distabanjong, K. and Geneve, R. L., *Plant Cell Rep.*, 1997, **16**, 334–338.
- Gharyal, P. K. and Maheshwari, S. C., *Naturwissenschaften*, 1981, **68**, 379–380.
- Rao, M. M. and Lakshmi Sita, G., *Plant Cell Rep.*, 1996, **15**, 355–359.
- Wetzstein, H. Y. and Baker, C. M., *Plant Sci.*, 1993, **92**, 81–89.
- McKently, A. H., Moore, G. A., Doostdar, H. and Niedz, R. P., *Plant Cell Rep.*, 1995, **14**, 699–703.
- Pena, L., Cervera, M., Juarez, J., Navarro, A., Pina, J. A. and Navarro, L., *Plant Cell Rep.*, 1997, **16**, 731–737.
- Fari, M., Nagy, I., Csanyi, M., Mityko, J. and Andrasfalvy, A., *Plant Cell Rep.*, 1995, **15**, 82–86.
- Akama, K., Shiraishi, H., Ohta, S., Nakamura, K., Okada, K. and Shimura, Y., *Plant Cell Rep.*, 1992, **12**, 7–11.
- Muthukumar, B., Mariamma, M., Veluthambi, K. and Gnanam, A., *Plant Cell Rep.*, 1996, **15**, 980–985.
- Kar, S., Johnson, T. M., Nayak, P. and Sen, S. K., *Plant Cell Rep.*, 1996, **16**, 32–37.